

# Obesity Blunts the Effect of Mesenchymal Stem Cell-Derived Extracellular Vesicles



Weijun Huang<sup>1,2,4</sup>, Siting Hong<sup>1,3,4</sup>, Xiangyang Zhu<sup>1</sup>, Mina H. Alsaedi<sup>1</sup>, Hui Tang<sup>1</sup>, James D. Krier<sup>1</sup>, Deep Gandhi<sup>1</sup>, Kyra L. Jordan<sup>1</sup>, Ishran M. Saadiq<sup>1</sup>, Yamei Jiang<sup>1</sup>, Alfonso Eirin<sup>1</sup> and Lilach O. Lerman<sup>1</sup>

<sup>1</sup>Division of Nephrology and Hypertension, Mayo Clinic, Rochester, Minnesota, USA; <sup>2</sup>Key Laboratory of Chinese Internal Medicine of Ministry of Education and Beijing, Dongzhimen Hospital Affiliated to Beijing University of Chinese Medicine, Beijing University of Chinese Medicine, Beijing, China; and <sup>3</sup>Department of Cardiology, The First Affiliated Hospital of Harbin Medical University, Harbin, China

**Introduction:** Mesenchymal stem/stromal cell-derived extracellular vesicles (MSC-EVs) are paracrine vectors with therapeutic functions comparable to their parent cells. However, it remains unclear if donor obesity affects their therapeutic functions. We tested the hypothesis that the curative effect of human adipose tissue-derived MSC-EVs (A-MSC-EVs) is blunted by obesity.

**Methods:** MSC-EVs were isolated by ultracentrifugation from mesenchymal stem/stromal cells (MSCs) collected from abdominal subcutaneous fat of obese and lean human subjects (obese and lean-MSC-EVs, respectively) and injected into the aorta of mice 2 weeks after renal artery stenosis (RAS) induction. Magnetic resonance imaging studies were conducted 2 weeks after MSC-EVs delivery to determine renal function. The effect of MSC-EVs on tissue injury was assessed by histology and gene expression of inflammatory factors, including interleukin (IL)-1 $\beta$ , IL-6, monocyte chemoattractant protein-1 (MCP-1), and tumor necrosis factor alpha (TNF- $\alpha$ ). Oxidative damage, macrophage infiltration, plasma renin, and hypoxia inducible factor-1 $\alpha$  (HIF-1 $\alpha$ ) were also assessed.

**Results:** Tracking showed that MSC-EVs localized in the kidney tissue, including glomeruli and tubules. All MSC-EVs decreased systolic blood pressure (SBP) and plasma renin and improved the poststenotic kidney (STK) volume, but obese-MSC-EVs were less effective than lean-MSC-EVs in improving medullary hypoxia, fibrosis, and tubular injury. Lean-MSC-EVs decreased inflammation, whereas obesity attenuated this effect. Only lean-MSC-EVs decreased STK cortical HIF-1 $\alpha$  expression.

**Conclusion:** Obesity attenuates the antihypoxia, antifibrosis, antiinflammation, and tubular repair functions of human MSC-EVs in chronic ischemic kidney disease. These observations may have implications for the self-repair potency of obese subjects and for the use of autologous MSC-EVs in regenerative medicine.

*Kidney Int Rep* (2023) 8, 1841–1851; <https://doi.org/10.1016/j.ekir.2023.06.009>

**KEYWORDS:** chronic kidney disease; extracellular vesicle; mesenchymal stem cell; obesity; regenerative medicine; stenotic kidney

© 2023 International Society of Nephrology. Published by Elsevier Inc. This is an open access article under the CC BY-NC-ND license (<http://creativecommons.org/licenses/by-nc-nd/4.0/>).

MSCs are considered a promising regenerative medicine because of their self-renewal, pluripotency, and immunomodulatory properties,<sup>1,2</sup> and can be derived from various tissues, such as fat, bone marrow, umbilical cord vein, and solid organs. MSC-EVs inherit some effective therapeutic functions of their parent cells<sup>3</sup>; however, they may pose a lower

risk of side effects<sup>4</sup> incurred by MSCs transplantation, such as tumorigenesis and thrombosis. Moreover, research studies, including a clinical trial showed that MSC-EVs exerted beneficial tissue regeneration and repair.<sup>5,6</sup> Our previous studies showed that porcine MSC-EVs preserved the post-STK microvasculature and attenuated kidney inflammation and fibrosis by inducing regulatory T-cells in pigs with metabolic syndrome and RAS, effects that exceeded those of renal revascularization.<sup>7–9</sup> Interestingly, a recent study showed that adipose MSC-EVs from young subjects can also hinder aging.<sup>10</sup>

Obesity is a major challenge for human health and can cause not only metabolic diseases, including

**Correspondence:** Lilach O. Lerman, Division of Nephrology and Hypertension, Mayo Clinic, 200 First Street SW, Rochester, Minnesota, 55905, USA. E-mail: [Lerman.Lilach@Mayo.Edu](mailto:Lerman.Lilach@Mayo.Edu)

<sup>4</sup>WH and SH contributed equally to this paper.

**Received 3 February 2023; revised 2 June 2023; accepted 12 June 2023; published online 21 June 2023**

hypertension, diabetes, and hyperlipidemia, but also cancer, inflammatory bowel diseases, and asthma. Notably, we have shown that obesity elicited adverse effects on adipose tissue-derived MSCs (A-MSC), such as mitochondrial dysfunction,<sup>11</sup> impaired immunomodulatory capacity,<sup>12</sup> and increased senescence.<sup>13</sup> The gene expression and miRNA signature were altered in obese porcine A-MSCs compared to healthy MSCs.<sup>14,15</sup> *In vivo* studies showed that obesity impairs the reparative properties of A-MSCs, possibly by inducing cellular senescence.<sup>16</sup> A modification of miRNA and mRNA by obesity was also observed in the cargo of A-MSC-EVs,<sup>17,18</sup> but its functional implications are unknown. Therefore, we hypothesized that obesity blunted the therapeutic effect of MSC-EVs in the chronically ischemic kidney.

## METHODS

### Animals

A total of 36 mice (of age 11 weeks, weight ~25 g) were randomized into 4 groups ( $n = 9$  mice each). The mice were housed with free access to water, under standard conditions (constant ambient temperature of 22 °C and humidity of 60% in a 12-h light/dark cycle). The animal protocol was approved by the Mayo Clinic Institute Animal Care and Use Committee. Unilateral RAS was induced as described previously.<sup>19</sup> Two weeks after RAS or sham surgery, MSC-EVs in 200  $\mu$ l of phosphate buffered saline (containing 30  $\mu$ g EVs, as prequantified by BCA assay) were injected into the aorta through the carotid artery. Blood pressure was measured by tail-cuff before and 2 weeks after EV injection. Magnetic resonance imaging studies were performed 2 weeks after injection following the protocol described previously<sup>20</sup> to assess the volume, oxygenation, and perfusion of the STK and left contralateral kidney. Renal volume was quantified with the images acquired by a respiration-gated 3-dimensional fast imaging with a steady precession sequence, and renal perfusion was measured using a flow-sensitive alternating inversion-recovery sequence. Blood oxygen level-dependent magnetic resonance imaging was performed using a respiration-gated 3-dimensional multiecho gradient-echo sequence to assess renal oxygenation. Urine was collected from the bladder and blood was drawn from the abdominal aorta, the mice were euthanized under anesthesia, and kidneys were collected and sectioned. Half of each kidney was fixed in 4% formalin, and the other half was flash-frozen and stored at  $-80^{\circ}\text{C}$ .

### MSCs Culture and EV Isolation

Human A-MSCs were used in this study. Individuals were recruited at Mayo clinic between October 2017

**Table 1.** Clinical characteristics of adipose tissue donors

Parameter	Lean	Obese
Demographics		
Number of subjects	7	7
Female sex	2/7	5/7
Caucasian Race	6/7	6/7
Age, yrs	59.57 $\pm$ 2.94	58.43 $\pm$ 4.09
Clinical:		
Body mass index, kg/m <sup>2</sup>	26.62 $\pm$ 1.33	43.13 $\pm$ 3.61 <sup>a</sup>
Systolic blood pressure, mm Hg	116.71 $\pm$ 8.31	135.33 $\pm$ 5.90
Diastolic blood pressure, mm Hg	75.43 $\pm$ 5.02	78.33 $\pm$ 3.00
Fasting blood glucose, mg/dl	93.67 $\pm$ 1.65	117.00 $\pm$ 13.32
Total cholesterol, mg/dl	191.50 $\pm$ 13.64	165.00 $\pm$ 28.95
Calculated LDL, mg/dl	115.50 $\pm$ 10.12	93.50 $\pm$ 20.96
Serum creatinine, mg/dl	1.30 $\pm$ 0.07	0.95 $\pm$ 0.09 <sup>b</sup>

LDL, low-density lipoprotein; ns, no significance.

<sup>a</sup> $P \leq 0.01$  vs. Lean.

<sup>b</sup> $P \leq 0.05$  vs. Lean.

and March 2019. Individuals with body mass index (BMI)  $<30$  kg/m<sup>2</sup> were considered to be lean, and subjects with BMI  $\geq 30$  kg/m<sup>2</sup> as obese. The mean ages of the lean and obese individuals were  $59.6 \pm 2.9$  and  $58.4 \pm 4.1$  years, respectively ( $P = 0.824$ ). Other characteristics are presented in Table 1. Abdominal subcutaneous fat (0.5 g–2.0 g) was collected with informed consent during bariatric or kidney donation surgeries to serve as obese or lean samples, respectively. All experimental study procedures were approved by Mayo Clinic Institutional Review Board. The process of subject recruitment, screening, enrollment, MSCs isolation, and characterization was previously described.<sup>13</sup> Markers such as CD73, CD90, and CD105 were detected in MSCs, which were also shown to differentiate into adipocytes, chondrocytes, and osteocytes, as previously described.<sup>21</sup> MSCs were cultured in Advanced Minimum Essential Medium supplemented with 5% platelet lysate (PLTmax, Rochester, MN; Mill Creek Life Sciences) and 1% glutamine (GlutaMax, Gibco) and amplified into T300 flasks. Media were collected for EV isolation when MSCs were confluent.

The EVs were isolated from MSC supernatants by ultracentrifugation, as previously described.<sup>22</sup> MSC supernatants were centrifuged at 2000 g for 20 minutes to remove cell fragments. Cell-free supernatants were transferred into a PA ULTRACRIMP tube (Thermo-scientific, 03990) and ultracentrifuged at 100,000 g for 1 hour at 4 °C. EVs were kept in the EV buffer and stored at  $-80^{\circ}\text{C}$ .

### EV Tracking

CellTrace Far Red Cell Proliferation kit (Part of ThermoFisher Scientific, Waltham, MA; Invitrogen, Cat. #C34564) was used to label EV before delivery as per

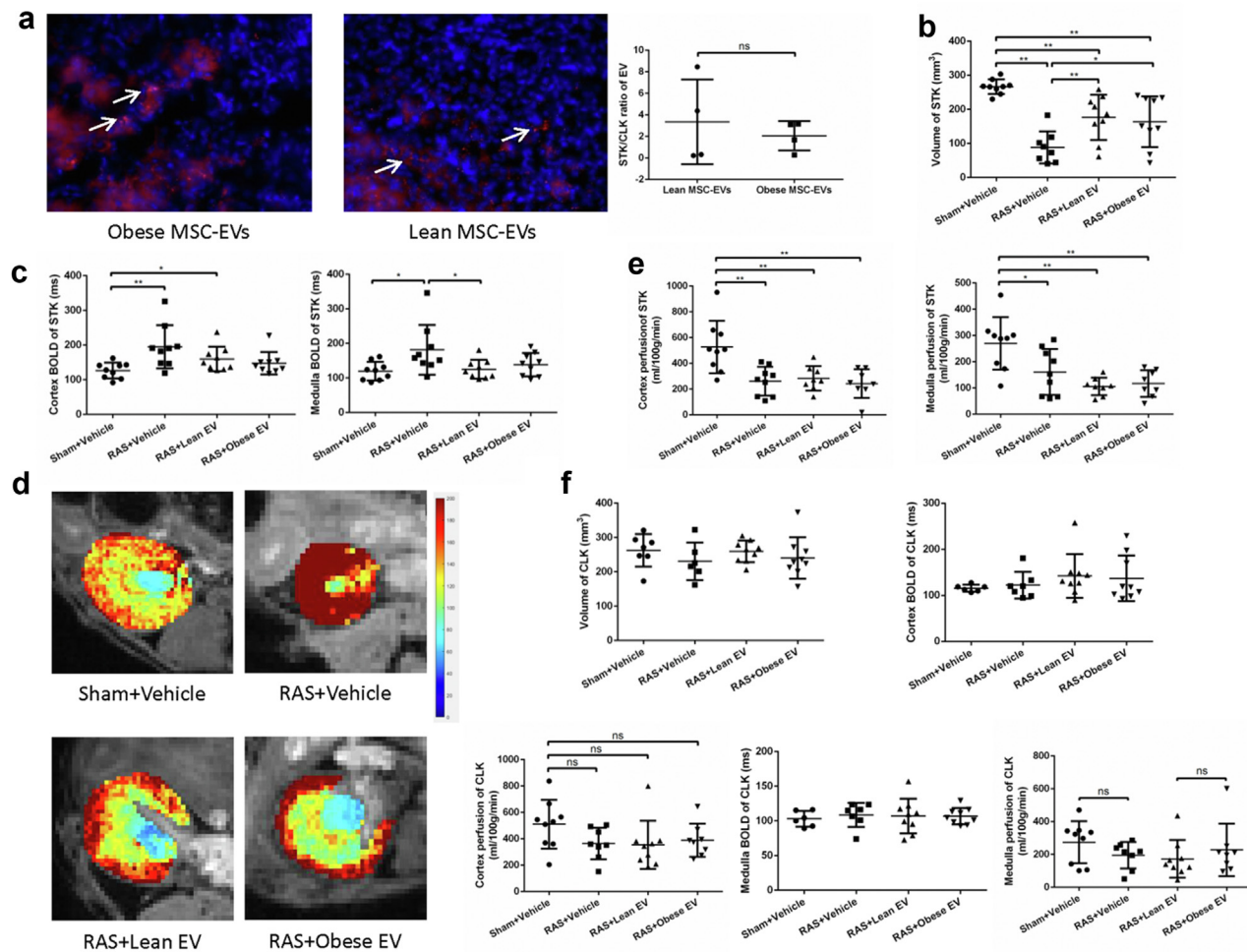


**Figure 1.** Effects of obese-MSC-EVs and lean-MSC-EVs on kidney volume, oxygenation, and perfusion. (a) Tracking showed that the ratios of lean- and obese-MSC-EV numbers were similar in the STK and CLK. (b) The volume, (c–d) oxygenation, and perfusion (e) assessed by MRI were all lower in the STK compared to the sham+vehicle kidneys. Lean- and obese-MSC-EVs improved the STK volume to a similar degree. Lean-MSC-EVs rescued the elevated medullary hypoxia ( $P < 0.05$ ) but not cortical hypoxia. Neither lean- nor obese-MSC-EVs restored the decreased perfusion. (f) RAS surgery and MSC-EVs treatment did not have significant effects on the volume, oxygenation, or perfusion of the CLK. \* $P < 0.05$ ; \*\* $P < 0.01$ . BOLD, blood oxygen level-dependent MRI; CLK, contralateral kidney; MRI, magnetic resonance imaging; MSC-EVs, mesenchymal stem/stromal cell-derived extracellular vesicles; ns, no significant difference; RAS, renal artery stenosis; STK, stenotic kidney.

the manufacturer's instructions. Frozen kidney sections (10  $\mu$ m) were stained with DAPI before taking images. Red dots (EV clusters) were counted in the STK and contralateral kidney, and the ratio was compared between lean-MSC-EVs and obese-MSC-EVs.

### Histological Staining

Kidney tissue was fixed with 4% paraformaldehyde for 24 hours and embedded with paraffin after gradient-alcohol dehydration, xylene vitrification, and waxdip. Masson's trichrome staining was conducted to assess renal fibrosis. Hematoxylin and eosin staining was used to assess tissue damage and score the tubular injury as previously described<sup>23</sup> on a scale 1 to 5 (1: <10%, 2: 10%–25%, 3: 26%–50%, 4: 51%–75% and 5: >75% injury). Immunohistochemistry was used to assess the expression of the oxidative stress marker 8-OHdG (sc-66036, 1:200), CD31 (DIA-310, 1:20) and of HIF-1 $\alpha$

(sc-13515, 1:200) in 5  $\mu$ m thick kidney tissue slides, following standard protocols. Immunofluorescence was performed to assess macrophage infiltration in kidney tissue with the marker F4/80 (Abcam, ab6640, 1:100).

### Real-Time Polymerase Chain Reaction

Total RNA was isolated from kidney tissue by mir Vana PARIS kit (ThermoFisher, AM1556). SuperScript VILO cDNA Synthesis kit (Waltham, MA; ThermoFisher Scientific, Cat#11754-050) was used to generate cDNA from 800 ng of total RNA. Relative quantitative polymerase chain reactions were performed using Taqman assays from ThermoFisher Scientific and the inflammatory primers IL-1 $\beta$  (mm00434228); IL-6 (mm00446190); MCP-1 (mm00441242); TNF- $\alpha$  (mm00443258); and GAPDH (mm99999915). Relative levels of mRNA were quantified and normalized to



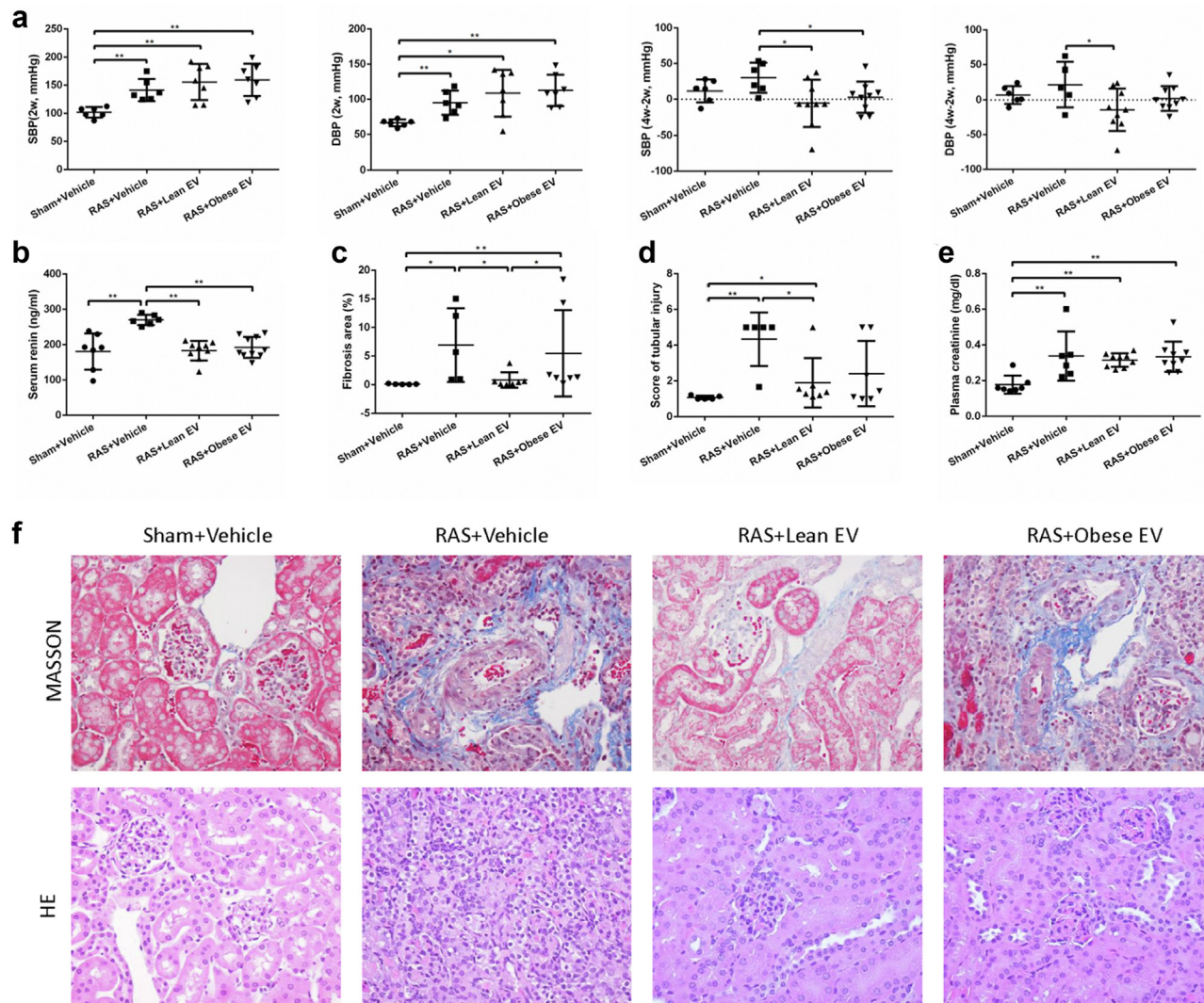


**Figure 2.** Effects of obese-MSC-EVs and lean-MSC-EVs on blood pressure, plasma renin content, plasma creatinine, and histological changes in the stenotic mouse kidney. (a) Blood pressure increased 2 weeks after RAS surgery ( $P < 0.01$ ); by 2 weeks after injection, systolic blood pressure (SBP) decreased by both lean- and obese-MSC-EVs ( $P < 0.05$ ), and diastolic blood pressure (DBP) only by lean-MSC-EVs ( $P < 0.05$ ). (b) Plasma renin was decreased by both types of EVs ( $P < 0.01$ ), suggesting the regulation of the renin-angiotensin-aldosterone system. (c,f) Masson's trichrome staining assessed renal fibrosis and only lean-MSC-EVs rescued the elevated fibrosis in STK ( $P < 0.05$ ). (d, f) Only lean-MSC-EVs attenuated tubular injury score in RAS ( $P < 0.05$ ), evaluated based on H&E staining. (e) Plasma creatinine was elevated by RAS ( $P < 0.01$ ) and unchanged by EVs. \* $P < 0.05$ ; \*\* $P < 0.01$ . H&E, hematoxylin and eosin; MSC-EVs, mesenchymal stem/stromal cell-derived extra-cellular vesicles; STK, stenotic kidney.

**Table 2.** Correlation of mouse characteristics with MSC donor BMI

Murine Recipient characteristics	R	P
Systolic blood pressure	0.140	0.634
Diastolic blood pressure	0.274	0.343
BOLD R2* (cortex)	-0.262	0.366
BOLD R2* (medulla)	0.236	0.416
Kidney volume	-0.182	0.533
Masson's trichrome staining	0.635	0.015
Tubular injury score	0.223	0.443
Perfusion (cortex)	-0.293	0.309
Perfusion (medulla)	0.222	0.446

BMI, body mass index; BOLD, Blood oxygen level-dependent; MSC, mesenchymal stem/stromal cell.

GAPDH mRNA by the  $2^{-\Delta\Delta CT}$  method. All polymerase chain reaction samples were run in duplicates.

### In Vitro Studies

Kidney tubular cell (LLC-PK1, ATCC) injury was induced by coculture with antimycin-A (10 ng/ml, Sigma) and TNF- $\alpha$  (10 ng/ml, R&D Systems) for 24 hours in a 24-well plate. EVs (30  $\mu$ g) were added into the medium at the beginning of the injury. Cell viability was evaluated using the 3-(4, 5-dimethylthiazol-2-yl)-5-(3-carboxymethoxyphenyl)-2-(4-sulfo-phenyl)-2H tetrazolium (to assess cell metabolic

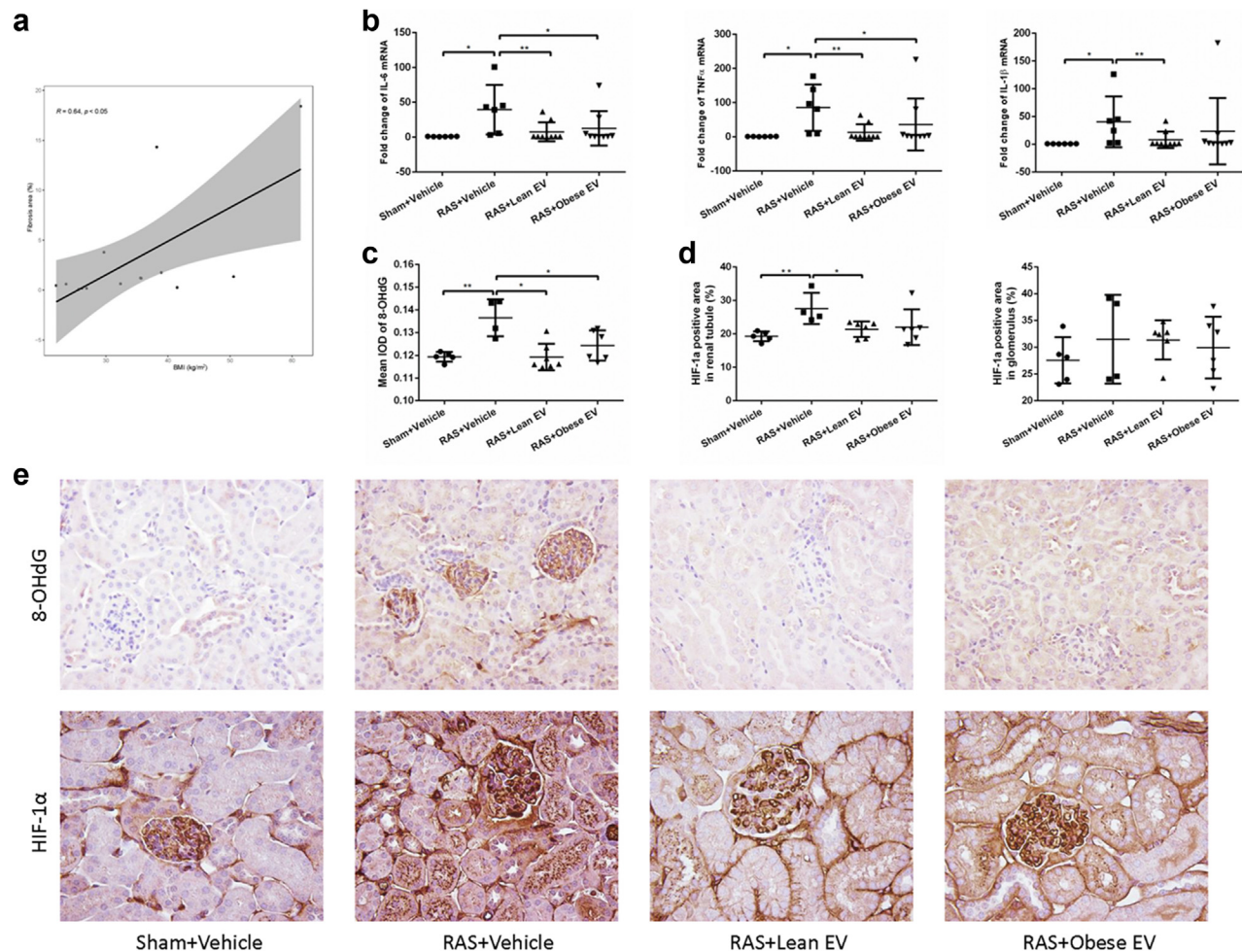


**Figure 3.** Effects of obese-MSC-EVs and lean-MSC-EVs on inflammation and oxidative damage. (a) The mRNA of IL-1 $\beta$ , IL-6, and TNF- $\alpha$  was quantified by quantitative polymerase chain reaction to assess the anti-inflammation effect of EVs. Both lean- and obese-MSC-EVs rescued the elevated TNF- $\alpha$  and IL-6 in the STK whereas only lean-MSC-EVs decreased IL-1 $\beta$  ( $P < 0.01$ ). (b–d) The immunoreactivity of 8-OHdG and HIF-1 $\alpha$  was detected by immunohistochemistry. 8-OHdG was downregulated by both lean and obese-MSC-EVs ( $P < 0.05$ ). HIF-1 $\alpha$  was only elevated in cortical tubules and rescued by lean-MSC-EVs ( $P < 0.05$ ). \* $P < 0.05$ ; \*\* $P < 0.01$ . IL, interleukin; TNF- $\alpha$ , tumor necrosis factor alpha; HIF-1 $\alpha$ , hypoxia inducible factor-1 $\alpha$ ; MSC-EVs, mesenchymal stem/stromal cell-derived extracellular vesicles; STK, stenotic kidney.

activity) and crystal violet (which assesses adherence of live cells) assays.

For migration assay, mice macrophages (RAW264.7, ATCC) were seeded into a 24-well plate. Scratch was made using an auto-scratcher (BioTek; BioTel Instruments, Agilent Technologies, Winooski, VT) when the cells reached 90% confluent, and then EVs (30  $\mu$ g) were added with or without an MCP-1 inhibitor (RS504393, 10  $\mu$ M, Sigma) and cultured for 48 hours in the Cytation-5 instrument (BioTek). Images were taken every 2 hours to assess the number of macrophages migrating across the scratch “wound.”

In addition, another set of RAW264.7 cells was seeded in chamber slides and cultured with EVs with or without the MCP-1 inhibitor for 24 hours. Immunostaining for MCP-1 (cat#NBP2-22115, Novus-Biologicals, 1:200 dilution) and TNF- $\alpha$  (cat#sc-8301, Santa-Cruz, 1:50 dilution) was then performed.

## Statistical Analysis

IBM SPSS Statistics 20.0 was used to analyze statistical differences among the groups. A normality test was conducted before statistical tests. Normally distributed data are shown as means  $\pm$  standard error and were analyzed using  $t$ -test, 1-way analysis of variance, or Pearson correlation, and nonnormally distributed data were analyzed by nonparametric tests or Spearman correlation. Enumeration data were analyzed with the  $\chi^2$  test. Statistically significant differences were accepted for  $P \leq 0.05$ .

## RESULTS

### Obese-MSC-EVs Were Less Effective Than Lean-MSC-EVs in the STK

To localize MSC-EVs in the kidney tissue, we pre-labeled them with a red fluorescent probe. Lean-MSC-



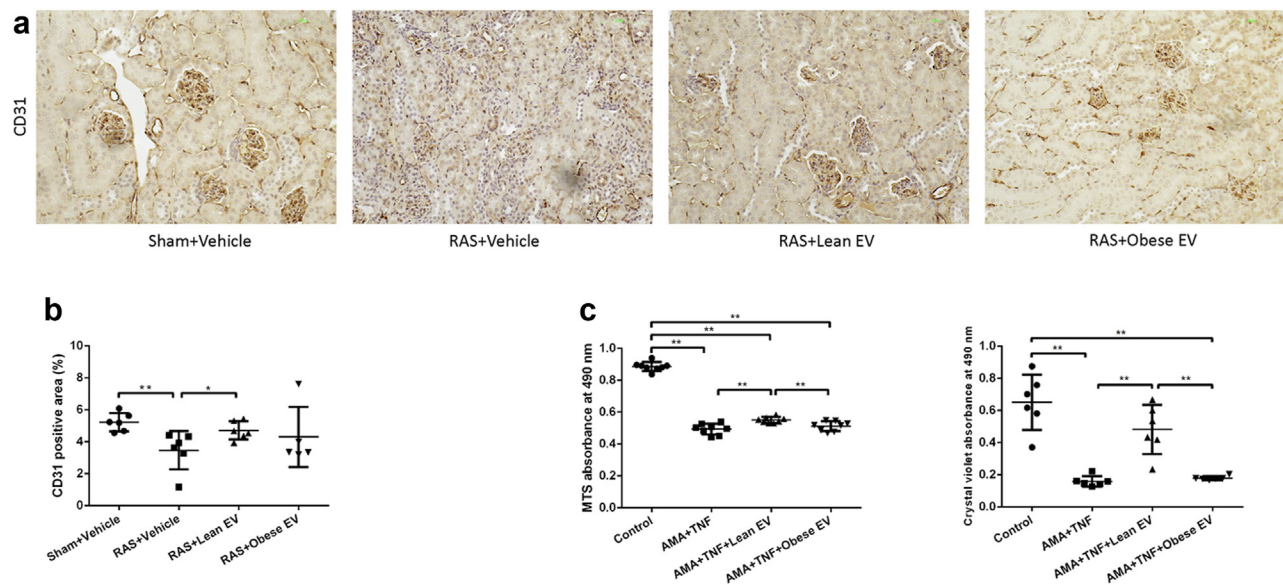


**Figure 4.** Potency of obese-MSC-EVs and lean-MSC-EVs in promoting angiogenesis and protecting PK-1 tubular cells. (a–b) Only lean-MSC-EVs, but not obese-MSC-EVs, increased the immunoreactivity of the vascular marker CD31 in the stenotic mouse kidney. (c) Both the MTS (3-(4,5-dimethylthiazol-2-yl)-5-(3-carboxymethoxyphenyl)-2-(4-sulfophenyl)-2H-tetrazolium) (cell proliferation) and crystal violet (cell viability) assays showed that only lean-MSC-EVs protect PK-1 cells from injury by antimycin-A and TNF- $\alpha$ . \* $P < 0.05$ ; \*\* $P < 0.01$ . TNF- $\alpha$ , tumor necrosis factor alpha.

EVs and obese-MSC-EVs showed no significant difference in engraftment and distribution between the STK and contralateral kidney. MSC-EV clusters (red dots) were observed in both the renal tubular and glomerular compartments (Figure 1a). Magnetic resonance imaging showed that both lean-MSC-EVs and obese-MSC-EVs improved the STK volume to a similar degree, though both remained lower than sham (Figure 1b). Interestingly, medullary hypoxia that was elevated in the STK was rescued by lean-MSC-EVs, whereas cortical hypoxia remained higher than normal after lean-MSC-EVs but not obese-MSC-EVs treatment (Figure 1c and d). In contrast, neither lean-MSC-EVs nor obese-MSC-EVs succeeded in improving the decreased STK perfusion (Figure 1e). In the contralateral kidney, no significant change in volume, oxidation, or perfusion was observed after RAS surgery or EV injection (Figure 1f). Both SBP and diastolic blood pressure increased 2 weeks after RAS surgery (Figure 2a). By 4 weeks after RAS surgery (2 weeks after EV injection), SBP was decreased by both lean-MSC-EVs and obese-MSC-EVs, whereas diastolic blood pressure was significantly decreased only by lean-MSC-EVs (Figure 2a). Plasma renin content that was elevated in untreated RAS mice was also decreased by both lean-MSC-EVs and obese-MSC-EVs and was no longer higher than normal (Figure 2b). In contrast, Masson's trichrome staining showed that lean-MSC-EVs relieved STK fibrosis, whereas obese-MSC-EVs did not (Figure 2c and f). The tubular injury score showed a similar trend, except that in RAS+Obese EVs

it was no longer higher than normal (Figure 2d and f). However, both lean-MSC-EVs and obese-MSC-EVs failed to improve the elevated plasma creatinine in the murine RAS model (Figure 2e). Therefore, obese-MSC-EVs were less effective than lean-MSC-EVs in decreasing blood pressure and improving STK fibrosis and tubular injury.

Furthermore, we analyzed if the BMI independently affected the therapeutic effects of MSC-EVs. The results of correlation analysis between BMI and SBP, diastolic blood pressure, blood oxygen level-dependent, volume (Table 2), Masson's trichrome staining, tubular injury score, and perfusion showed that only the area of positive Masson's trichrome staining had a significant direct correlation with the donor BMI (Spearman correlation coefficient  $r_s = 0.635$ ,  $P = 0.015$ ) (Figure 3a). The donor characteristics, including age, gender, race, blood pressure, fasting blood glucose, total cholesterol, and calculated low-density lipoprotein, showed no significant difference between the lean and obese groups except for BMI and serum creatinine (Table 1). In addition, results of stepwise regression analysis between the area of positive Masson's trichrome staining and BMI, age, blood pressure, fasting blood glucose, total cholesterol, calculated low-density lipoprotein, and serum creatinine showed that only BMI significantly affected the area of positive Masson's trichrome staining (Constant =  $-9.043$ ,  $B = 0.337$ , adjusted  $R^2 = 0.532$ ,  $P = 0.007$ ). Therefore, BMI independently affected the antifibrosis function of MSC-EVs.

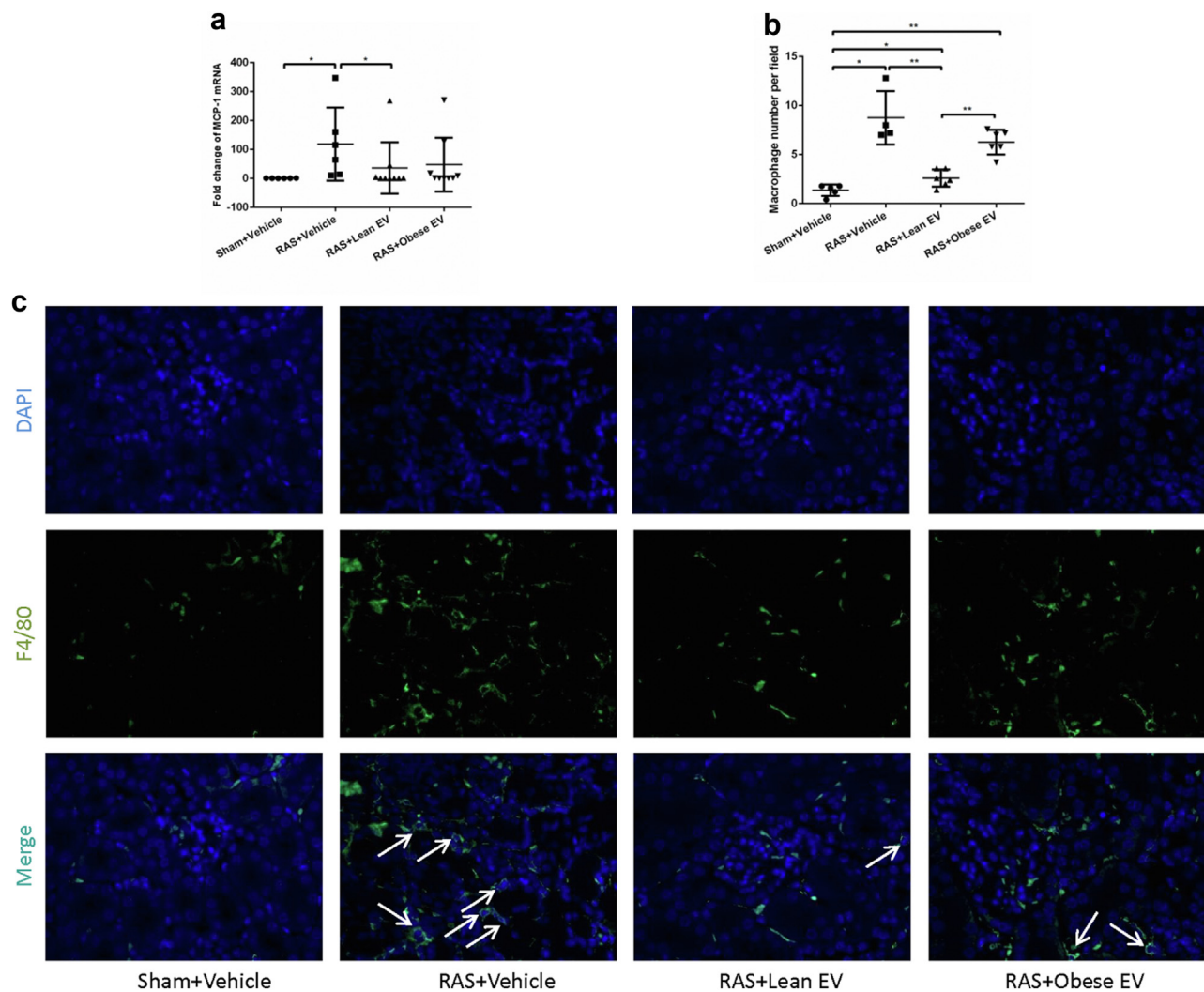


**Figure 5.** Potency of obese and lean-MSC-EVs in suppressing macrophage infiltration. (a) Only lean-MSC-EVs downregulated the elevated MCP-1 mRNA expression in the stenotic mouse kidney (STK). (b–c) Macrophages stained by F4/80 were detected by immunofluorescence. A greater number of macrophages was observed in the STK, which was restored only by lean-MSC-EVs compared to both RAS+vehicle and RAS+obese-MSC-EVs. \* $P < 0.05$ ; \*\* $P < 0.01$ .

### Lean-MSC-EVs Showed Better Antiinflammation and Antioxidative Effects Than Obese-MSC-EVs

Polymerase chain reaction showed that IL-6 and TNF- $\alpha$  mRNA expression was upregulated in the STK and rescued by both lean-MSC-EVs and obese-MSC-EVs, whereas only lean-MSC-EVs significantly decreased IL-1 $\beta$  mRNA expression (Figure 3b). In contrast, 8-OHdG which was overexpressed in the STK was downregulated by both lean-MSC-EVs and obese-MSC-EVs (Figure 3c and e). In the renal cortical tubules, HIF-1 $\alpha$  immunoreactivity was upregulated in RAS+Vehicle and was significantly lower in RAS+lean-MSC-EVs but not in the RAS+obese-MSC-EVs group. In contrast, RAS did not upregulate the expression of HIF-1 $\alpha$  in the glomeruli and neither lean-MSC-EVs nor obese-MSC-EVs had any effect (Figure 3d and e). The immunoreactivity of CD31, an endothelial cell marker, decreased

in RAS+Vehicle compared to sham, suggesting microvascular loss, and was upregulated by lean-MSC-EVs but not by obese-MSC-EVs (Figure 4a–b).

*In vitro*, lean-MSC-EVs relieved PK-1 injury caused by antimycin-A and TNF- $\alpha$ , whereas obese-MSC-EVs failed (Figure 4c). Cell viability (3-(4, 5-dimethylthiazol-2-yl)-5-(3-carboxymethoxyphenyl)-2-(4-sulfo-phenyl)-2H tetrazolium) was improved, though not normalized, whereas cell adherence (crystal violet) was no longer different from control after coculture with lean-MSC-EVs.

### Lean-MSC-EVs Ameliorated Macrophage Infiltration Better Than Obese-MSC-EVs

MCP-1 can induce macrophage infiltration and inflammation.<sup>24</sup> In the STK, MCP-1 mRNA expression increased, and macrophage infiltration was evident (Figure 5). Lean-MSC-EVs significantly suppressed

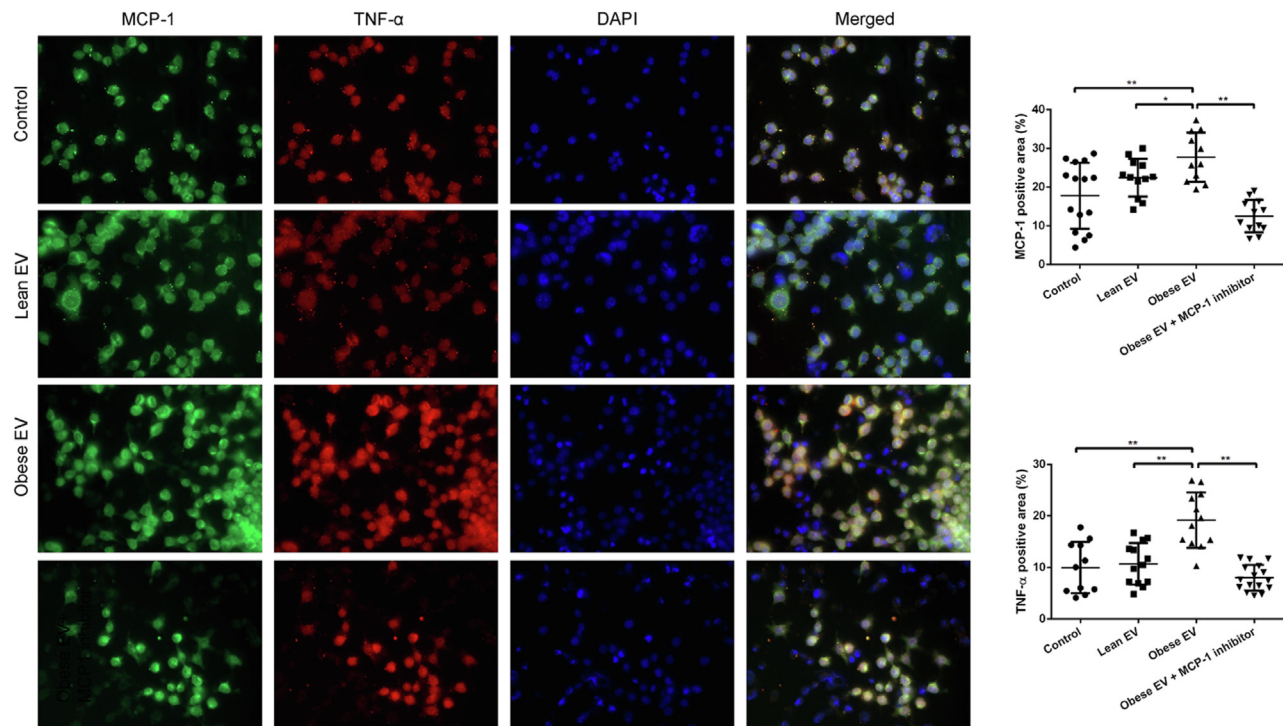


**Figure 6.** Effect of obese and lean-MSC-EVs on TNF- $\alpha$  and MCP-1 obese-MSC-EVs increased the expression of TNF- $\alpha$  and MCP-1, but lean-MSC-EVs didn't. TNF- $\alpha$  decreased in obese-MSC-EVs treated-macrophage when MCP-1 was inhibited. \* $P < 0.05$ ; \*\* $P < 0.01$ . MCP-1, monocyte chemotactic protein-1; MSC-EVs, mesenchymal stem/stromal cell-derived extracellular vesicles; TNF- $\alpha$ , tumor necrosis factor alpha.

expression of MCP-1 mRNA (Figure 5a) and inhibited macrophage infiltration (Figure 5b and c), though it remained higher than in sham. In contrast, in RAS+obese MSC-EVs MCP-1 expression was not different from RAS (Figure 5a), and macrophage numbers remained unchanged (Figure 5b and c). An *in vitro* study showed that MCP-1 and TNF- $\alpha$  expression was increased in obese-MSC-EVs-treated macrophages, and TNF- $\alpha$  expression declined when cultured with an MCP-1 inhibitor (Figure 6). A similar trend was observed in the migration study. Obese-MSC-EVs promoted macrophage migration compared with lean-MSC-EVs, whereas obese-MSC-EVs + MCP-1 did not (Figure 7).

## DISCUSSION

This study shows that MSC-derived EVs obtained from fat tissue of obese patients are less effective than those obtained from lean subjects in repairing injured mouse kidneys *in vivo* or tubular cells *in vitro*. This study, therefore, highlights an important functional deficit in these MSC vectors, which is consistent with impaired reparative potency in obesity.

Chronic ischemic nephropathy is an important cause of end-stage renal disease. Accumulating evidence has indicated that MSC-EVs are a promising therapy for kidney diseases, including chronic ischemic

nephropathy.<sup>25</sup> However, many of these patients are also affected by obesity, which as our previous studies showed may alter the cargoes of MSC-EVs.<sup>18</sup> We previously compared the effects of lean and obese A-MSCs in a mouse model of chronic ischemic nephropathy and found that lean but not obese A-MSCs decreased macrophage infiltration and downregulated inflammatory factors (such as TNF- $\alpha$ , MCP-1, IL-1 $\alpha$ , and IL-6) in the kidney tissue.<sup>12</sup> MSC-EVs have similar functions to their parent cells because increasing studies have shown their ability to attenuate inflammation and senescence and improve tissue repair.<sup>25,26</sup> We, therefore, hypothesized that obesity blunts the functions of MSC-EVs as well.

In this study, obese-MSC-EVs had the same efficacy as lean-MSC-EVs in improving STK volume and decreasing SBP and plasma renin but not in improving medullary hypoxia, diastolic blood pressure, fibrosis, angiogenesis, or tubular injury. Interestingly, immunohistochemistry showed upregulation of HIF-1 $\alpha$  only in cortical tubules but not in glomeruli, which contributes to the progression of renal fibrosis,<sup>27</sup> and only lean-MSC-EVs successfully downregulated it. The discrepant expression may be because the glomerulus has a relatively rich blood supply and glomerular cells might be able to adapt to chronic ischemia, unlike the tubulointerstitium and medulla. This also can explain why lean-MSC-EVs have a more significant effect on



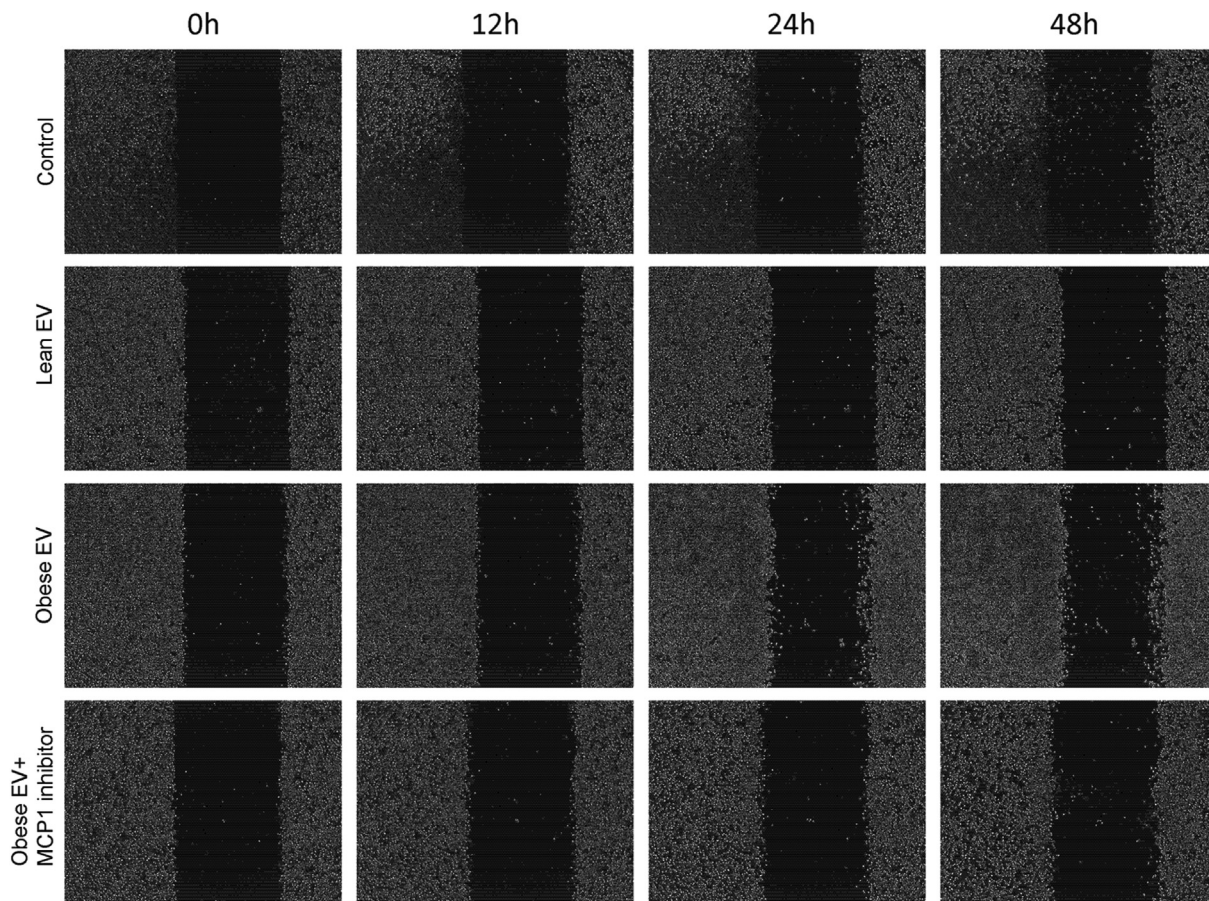


**Figure 7.** Effect of obese and lean-MSC-EVs on macrophage migration. The wound scratch study showed that compared to control and lean-MSC-EVs obese-MSC-EVs promoted macrophage migration, which was blunted by an MCP-1 inhibitor. \* $P < 0.05$ . MCP-1, monocyte chemoattractant protein-1; MSC-EVs, mesenchymal stem/stromal cell-derived extracellular vesicles.

medullary hypoxia. Notably, HIF-1 $\alpha$  can also target the angiotensin receptor,<sup>28</sup> which might explain why obese-MSC-EVs had a lesser effect on lowering blood pressure despite decreasing plasma renin as effectively as lean-MSC-EVs. Interestingly, neither lean-MSC-EVs nor obese-MSC-EVs improved kidney perfusion and plasma creatinine, possibly because of the short intervention time. Yet, taken together, these results indicated that obesity blunted the antihypoxia, antifibrosis, and tubulo-protective capacity of MSC-EVs. Notably, the ability of MSC-EVs to blunt murine STK fibrosis was inversely correlated with the human donor BMI, again linking obesity with impaired MSC-EVs function.

Chronic ischemic nephropathy can magnify reactive oxygen species production and oxidative damage to kidney cells.<sup>29</sup> This in turn can induce overexpression of MCP-1, which then attracts macrophage infiltration in the kidney, resulting in chronic inflammation and fibrosis.<sup>24,30,31</sup> In this study, we found evidence of oxidative damage, upregulation of MCP-1, IL-1 $\beta$ , IL-6, and TNF- $\alpha$  mRNA, macrophage infiltration, fibrosis, increased blood pressure and plasma creatinine, and

STK atrophy, which are consistent with ischemic damage. Notably, lean-MSC-EVs relieved the oxidative damage, rescued the increased inflammatory factors, and suppressed macrophage infiltration, whereas obese-MSC-EVs failed to suppress macrophage infiltration and mRNA expression of MCP-1 or IL-1 $\beta$ . Consistent with the *in-vivo* study, only lean-MSC-EVs protected PK-1 from injury induced by antimycin-A and TNF- $\alpha$ . Further, obese MSC-EVs promoted the expression of TNF- $\alpha$  and macrophage migration, which were attenuated when MCP-1 was inhibited. These results indicated that their antiinflammation and anti-macrophage function might be dependent on MCP-1 signaling.

Apparently, obesity blunted the reparative effect of MSC-EVs. This may have been secondary to the alteration of immunomodulation-related properties of their parent MSCs<sup>12</sup> and in turn EV cargoes, including mRNAs, micro-RNAs, and proteins, which we had previously characterized. For example, applying transcriptome and proteome studies, we have shown that obesity upregulated in A-MSC-EVs, the signaling of TNF- $\alpha$ , NF $\kappa$ -B, and MAPK, and inflammation mediated

by chemokines and cytokines, and that coculture with obese-MSC-EVs increased renal tubular cell inflammation *in vitro*.<sup>18,32,33</sup> Moreover, we have demonstrated that obesity interferes with the packaging of proteins within MSC-EVs. Proteins related to acute inflammatory responses, leukocyte trans-endothelial migration, and cytokine production were all enriched in obese-MSC-EVs.<sup>34</sup> The current study extends our previous observations by showing that these cargo alterations have functional ramifications on the reparative potency of EVs *in vivo*. Overall, these findings show that obesity blunts the antiinflammation capability of MSC-EVs, especially in suppressing macrophage infiltration.

However, this study had some limitations. First, ultracentrifugation that was used to isolate the EVs might have affected their purity. Second, the injection dose was calculated based on the protein volume of the EV solution, which may contain protein not only within but also outside the vesicles. Third, a single dose was injected during a period of 2-week observation. This may affect the efficacy of MSC-EVs and may account for their lack of efficacy to improve perfusion and plasma creatinine.

In conclusion, obesity should be considered when using autologous adipose tissue MSC-EVs as a regenerative strategy. Future studies need to target key factors affecting EV functions, such as their cargo, and thus engineering improved EVs. For example, transfecting MSCs with specific miRNA mimics might increase their effectiveness in treating acute kidney injury.<sup>35</sup> Alternatively, pretreatment of the parent MSCs with drugs<sup>36</sup> (e.g., antiinflammatory, anti-senescence, or antioxidant drugs) or specific culture conditions<sup>37</sup> (e.g., hypoxic preconditioning) might restore the function of MSC-EVs derived from adipose tissue of obese subjects. In addition, MSC-EVs injected via the peripheral circulation localized not only in the kidney but also in other organs and tissues. Specific targeting techniques may improve their effectiveness and decrease off-target effects.<sup>38</sup> Further studies are also needed to improve the function of the endogenous MSC and their daughter EVs<sup>13</sup> in obese subjects *in situ* to improve their capacity for self-healing.

## DISCLOSURE

LOL is an advisor to AstraZeneca, CureSpec, and Ribocure Pharmaceuticals. All other authors declared no competing interest.

## ACKNOWLEDGMENT

### Funding

This study was partly supported by NIH grant numbers: DK120292, DK122734, HL158691, and AG062104.

## Data Availability

The data that supports this study is available from the corresponding authors upon reasonable request.

## REFERENCES

1. Wu X, Jiang J, Gu Z, Zhang J, Chen Y, Liu X. Mesenchymal stromal cell therapies: immunomodulatory properties and clinical progress. *Stem Cell Res Ther*. 2020;11:345. <https://doi.org/10.1186/s13287-020-01855-9>
2. Noronha NC, Mizukami A, Caláiri-Oliveira C, et al. Priming approaches to improve the efficacy of mesenchymal stromal cell-based therapies. *Stem Cell Res Ther*. 2019;10:131. <https://doi.org/10.1186/s13287-019-1224-y>
3. He J, Wang Y, Lu X, et al. Micro-vesicles derived from bone marrow stem cells protect the kidney both in vivo and in vitro by microRNA-dependent repairing. *Nephrol (Carlton)*. 2015;20:591–600. <https://doi.org/10.1111/nep.12490>
4. Zhai M, Zhu Y, Yang M, Mao C. Human mesenchymal stem cell derived exosomes enhance cell-free bone regeneration by altering their miRNAs profiles. *Adv Sci (Weinh)*. 2020;7: 2001334. <https://doi.org/10.1002/advs.202001334>
5. Matsuzaka Y, Yashiro R. Therapeutic strategy of mesenchymal-stem-cell-derived extracellular vesicles as regenerative medicine. *Int J Mol Sci*. 2022;23. <https://doi.org/10.3390/ijms23126480>
6. Nassar W, El-Ansary M, Sabry D, et al. Umbilical cord mesenchymal stem cells derived extracellular vesicles can safely ameliorate the progression of chronic kidney diseases. *Biomater Res*. 2016;20:21. <https://doi.org/10.1186/s40824-016-0068-0>
7. Ferguson CM, Farahani RA, Zhu XY, et al. Mesenchymal stem/stromal cell-derived extracellular vesicles elicit better preservation of the intra-renal microvasculature than renal revascularization in pigs with renovascular disease. *Cells*. 2021;10. <https://doi.org/10.3390/cells10040763>
8. Eirin A, Zhu XY, Puranik AS, et al. Mesenchymal stem cell-derived extracellular vesicles attenuate kidney inflammation. *Kidney Int*. 2017;92:114–124. <https://doi.org/10.1016/j.kint.2016.12.023>
9. Song T, Eirin A, Zhu X, et al. Mesenchymal stem cell-derived extracellular vesicles induce regulatory T cells to ameliorate chronic kidney injury. *Hypertension*. 2020;75:1223–1232. <https://doi.org/10.1161/HYPERTENSIONAHA.119.14546>
10. Sanz-Ros J, Romero-García N, Mas-Bargues C, et al. Small extracellular vesicles from young adipose-derived stem cells prevent frailty, improve health span, and decrease epigenetic age in old mice. *Sci Adv*. 2022;8:eabq2226. <https://doi.org/10.1126/sciadv.abq2226>
11. Meng Y, Eirin A, Zhu XY, et al. Obesity-induced mitochondrial dysfunction in porcine adipose tissue-derived mesenchymal stem cells. *J Cell Physiol*. 2018;233:5926–5936. <https://doi.org/10.1002/jcp.26402>
12. Zhu XY, Klomjit N, Conley SM, et al. Impaired immunomodulatory capacity in adipose tissue-derived mesenchymal stem/stromal cells isolated from obese patients. *J Cell Mol Med*. 2021;25:9051–9059. <https://doi.org/10.1111/jcmm.16869>
13. Conley SM, Hickson LJ, Kellogg TA, et al. Human obesity induces dysfunction and early senescence in adipose tissue-



- derived mesenchymal stromal/stem cells. *Front Cell Dev Biol.* 2020;8:197. <https://doi.org/10.3389/fcell.2020.00197>
14. Conley SM, Zhu XY, Eirin A, et al. Metabolic syndrome alters expression of insulin signaling-related genes in swine mesenchymal stem cells. *Gene.* 2018;644:101–106. <https://doi.org/10.1016/j.gene.2017.10.086>
  15. Meng Y, Eirin A, Zhu XY, et al. The metabolic syndrome alters the miRNA signature of porcine adipose tissue-derived mesenchymal stem cells. *Cytom A.* 2018;93:93–103. <https://doi.org/10.1002/cyto.a.23165>
  16. Klomjit N, Conley SM, Zhu XY, et al. Effects of obesity on reparative function of human adipose tissue-derived mesenchymal stem cells on ischemic murine kidneys. *Int J Obes (Lond).* 2022;46:1222–1233. <https://doi.org/10.1038/s41366-022-01103-5>
  17. Li Y, Meng Y, Zhu X, et al. Metabolic syndrome increases senescence-associated micro-RNAs in extracellular vesicles derived from swine and human mesenchymal stem/stromal cells. *Cell Commun Signal.* 2020;18:124. <https://doi.org/10.1186/s12964-020-00624-8>
  18. Eirin A, Meng Y, Zhu XY, et al. The micro-RNA cargo of extracellular vesicles released by human adipose tissue-derived mesenchymal stem cells is modified by obesity. *Front Cell Dev Biol.* 2021;9:660851. <https://doi.org/10.3389/fcell.2021.660851>
  19. Zhu XY, Zou X, Mukherjee R, et al. Targeted imaging of renal fibrosis using antibody-conjugated gold nanoparticles in renal artery stenosis. *Invest Radiol.* 2018;53:623–628. <https://doi.org/10.1097/RLI.0000000000000476>
  20. Jiang K, Ferguson CM, Ebrahimi B, et al. Noninvasive assessment of renal fibrosis with magnetization transfer MR imaging: validation and evaluation in murine renal artery stenosis. *Radiology.* 2017;283:77–86. <https://doi.org/10.1148/radiol.2016160566>
  21. Zhu XY, Ma S, Eirin A, et al. Functional plasticity of adipose-derived stromal cells during development of obesity. *Stem Cells Transl Med.* 2016;5:893–900. <https://doi.org/10.5966/sctm.2015-0240>
  22. Eirin A, Riester SM, Zhu XY, et al. MicroRNA and mRNA cargo of extracellular vesicles from porcine adipose tissue-derived mesenchymal stem cells. *Gene.* 2014;551:55–64. <https://doi.org/10.1016/j.gene.2014.08.041>
  23. Ebrahimi B, Eirin A, Li Z, et al. Mesenchymal stem cells improve medullary inflammation and fibrosis after revascularization of swine atherosclerotic renal artery stenosis. *PLoS One.* 2013;8:e67474. <https://doi.org/10.1371/journal.pone.0067474>
  24. Du Z, Wu X, Song M, Li P, Wang L. Oxidative damage induces MCP-1 secretion and macrophage aggregation in age-related macular degeneration (AMD). *Graefes Arch Clin Exp Ophthalmol.* 2016;254:2469–2476. <https://doi.org/10.1007/s00417-016-3508-6>
  25. Huang W, Zhu XY, Lerman A, Lerman LO. Extracellular vesicles as theranostic tools in kidney disease. *Clin J Am Soc Nephrol.* 2022;17:1418–1429. <https://doi.org/10.2215/CJN.16751221>
  26. Huang W, Hickson LJ, Eirin A, Kirkland JL, Lerman LO. Cellular senescence: the good, the bad and the unknown. *Nat Rev Nephrol.* 2022;18:611–627. <https://doi.org/10.1038/s41581-022-00601-z>
  27. Kimura K, Iwano M, Higgins DF, et al. Stable expression of HIF-1 $\alpha$  in tubular epithelial cells promotes interstitial fibrosis. *Am J Physiol Ren Physiol.* 2008;295:F1023–F1029. <https://doi.org/10.1152/ajprenal.90209.2008>
  28. Yu J, Wang S, Shi W, et al. Roxadustat prevents Ang II hypertension by targeting angiotensin receptors and eNOS. *JCI Insight.* 2021;6. <https://doi.org/10.1172/jci.insight.133690>
  29. Kimlinger MJ, Mace EH, Harris RC, et al. Impact of inhaled oxygen on reactive oxygen species production and oxidative damage during spontaneous ventilation in a murine model of acute renal ischemia and reperfusion. *Med Res Arch.* 2021;9:2575. <https://doi.org/10.18103/mra.v9i10.2575>
  30. Sung FL, Zhu TY, Au-Yeung KK, Siow YL, O K. Enhanced MCP-1 expression during ischemia/reperfusion injury is mediated by oxidative stress and NF- $\kappa$ B. *Kidney Int.* 2002;62:1160–1170. <https://doi.org/10.1111/j.1523-1755.2002.kid577.x>
  31. Shimizu H, Bolati D, Higashiyama Y, Nishijima F, Shimizu K, Niwa T. Indoxyl sulfate upregulates renal expression of MCP-1 via production of ROS and activation of NF- $\kappa$ B, p53, ERK, and JNK in proximal tubular cells. *Life Sci.* 2012;90:525–530. <https://doi.org/10.1016/j.lfs.2012.01.013>
  32. Pawar AS, Eirin A, Tang H, Zhu XY, Lerman A, Lerman LO. Upregulated tumor necrosis factor- $\alpha$  transcriptome and proteome in adipose tissue-derived mesenchymal stem cells from pigs with metabolic syndrome. *Cytokine.* 2020;130:155080. <https://doi.org/10.1016/j.cyto.2020.155080>
  33. Meng Y, Eirin A, Zhu XY, et al. The metabolic syndrome modifies the mRNA expression profile of extracellular vesicles derived from porcine mesenchymal stem cells. *Diabetol Metab Syndr.* 2018;10:58. <https://doi.org/10.1186/s13098-018-0359-9>
  34. Eirin A, Zhu XY, Woollard JR, et al. Metabolic syndrome interferes with packaging of proteins within porcine mesenchymal stem cell-derived extracellular vesicles. *Stem Cells Transl Med.* 2019;8:430–440. <https://doi.org/10.1002/sctm.18-0171>
  35. Tapparo M, Bruno S, Collino F, et al. Renal regenerative potential of extracellular vesicles derived from miRNA-engineered mesenchymal stromal cells. *Int J Mol Sci.* 2019;20:2381. <https://doi.org/10.3390/ijms20102381>
  36. Hickson LJ, Langhi Prata LGP, Bobart SA, et al. Senolytics decrease senescent cells in humans: preliminary report from a clinical trial of dasatinib plus quercetin in individuals with diabetic kidney disease. *EBiomedicine.* 2019;47:446–456. <https://doi.org/10.1016/j.ebiom.2019.08.069>
  37. Farooqui N, Mohan A, Isik B, et al. Effect of hypoxia preconditioning on the regenerative capacity of adipose tissue derived mesenchymal stem cells in a model of renal artery stenosis. *Stem Cells.* 2023;41:50–63. <https://doi.org/10.1093/stmcls/sxac073>
  38. Chen XJ, Jiang K, Ferguson CM, et al. Augmented efficacy of exogenous extracellular vesicles targeted to injured kidneys. *Signal Transduct Target Ther.* 2020;5:199. <https://doi.org/10.1038/s41392-020-00304-6>